Spectrochimica Acta Part A: Molecular and Biomolecular Spectroscopy 330 (2025) 125726

Contents lists available at ScienceDirect

Spectrochimica Acta Part A:
Molecular and Biomolecular Spectroscopy

journal homepage: www.journals.elsevier.com/spectrochimica-acta-part-a-molecular-and-biomolecular-spectroscopy

Deepening Cisplatin sensitivity on Oral Squamous cell Carcinoma cell lines after PON2 knockdown: A FTIRM investigation

Alessia Belloni [a,1], Roberto Campagna [b,1], Valentina Notarstefano [a], Valentina Pozzi [b], Giulia Orilisi [b], Veronica Pompei [b], Lucrezia Togni [b], Marco Mascitti [b], Davide Sartini [b,*], Elisabetta Giorgini [a,*], Andrea Santarelli [b], Monica Emanuelli [b]

[a] Dipartimento di Scienze della Vita e dell'Ambiente, Università Politecnica delle Marche Via Brecce Bianche 60131 Ancona, Italy
[b] Dipartimento di Scienze Cliniche, Specialistiche ed Odontostomatologiche, Università Politecnica delle Marche, Via Tronto 10/a 60020 Ancona, Italy

HIGHLIGHTS

- PON2 defends cells from the damages induced by Reactive Oxygen Species (ROS)
- In OTSCC, PON2 is involved in a resistance mechanism against Cisplatin (CDDP)
- Chemoresistance is linked to aggressiveness resulting in poor outcome.
- PON2 knockdown could represent a possible approach to escape the chemoresistance.
- FTIRM is a reliable tool to evaluate the efficacy of the improved sensitivity.

GRAPHICAL ABSTRACT

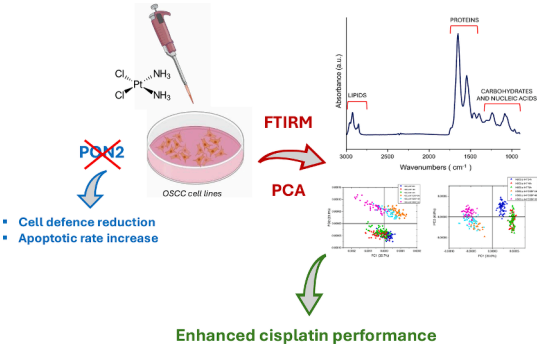

ARTICLE INFO

Keywords:
Oral Squamous Cell Carcinoma
Cisplatin
HOC621 cell lines
HSC-3 cell lines
Paraoxonase-2 (PON2)
Fourier-Transform Infrared Microspectroscopy
Multivariate analysis

ABSTRACT

Cisplatin is a platinum-based chemotherapy drug with antimicrobial and antitumoral activity, largely used for a long time in the treatment of several cancers, including the Oral Squamous Cell Carcinoma (OSCC), which is one of the most frequent neoplasms of the oral cavity. Due to its aggressiveness and metastatic invasion, OSCC is characterized by poor outcome, often related also to chemoresistance mechanisms. The intracellular enzyme paraoxonase-2 (PON2) normally acts defending cells from the damages induced by Reactive Oxygen Species. Hence, in cancer cells, this enzyme can shield the potential of cisplatin, triggering a resistance mechanism. Based on this evidence, PON2 knockdown seems to be a valuable way to enhance the effects of chemotherapy, escaping this resistance. In this study, HOC621 and HSC-3 OSCC cell lines submitted to PON2 silencing were analyzed by Fourier Transform Infrared Microspectroscopy to evaluate the time-dependent changes occurring in these cells after cisplatin treatment. Spectral data were statistically analyzed by multivariate and univariate analyses and compared with MTT results. Positive feedback on cisplatin efficacy was found in both cell lines submitted to

Abbreviations: CDDP, Cisplatin; FTIRM, Fourier Transform InfraRed Microspectroscopy; OSCC, Oral Squamous Cell Carcinoma; OTSCC, Oral Tongue Squamous Cell Carcinoma; PCA, Principal Component Analysis; PFA, Paraformaldehyde; PON2, Paraoxonase 2; ROS, Reactive Oxygen Species.

* Corresponding authors.
E-mail addresses: d.sartini@univpm.it (D. Sartini), e.giorgini@univpm.it (E. Giorgini).

[1] A.B and R.C equally contributed as first Authors.

https://doi.org/10.1016/j.saa.2025.125726
Received 24 April 2024; Received in revised form 29 November 2024; Accepted 6 January 2025
Available online 9 January 2025

PON2 knockdown, even if with a different response. In particular, a less growth was found in PON2 silenced HOC 621 cells, respect to HSC-3 ones. Moreover, specific spectral markers (A_{1172}/A_{TOT}, A_{1053}/A_{TOT}, A_{967}/A_{1080}, and A_{992}/A_{TOT} band area ratios) were identified and statistically analyzed ($p < 0.05$): cellular alterations mainly in nucleic acids and carbohydrates were found in both cell lines, although more evident in HOC 621 ones, which therefore appeared to be more affected by chemotherapy treatment.

1. Introduction

Oral Squamous Cell Carcinoma (OSCC), known as the most common carcinoma of the entire oral cavity, represents a malignancy affecting both men and women of different ages, especially in specific world countries such as India [1]. With the highest percentage in elder men accounting for 70 % and a slightly lower percentage of 50–65 % under 45 years of age, the incidence of this carcinoma seems to have increased in young people and generally in women in the last decades.

The main causes of incidence of the OSCC can be ascribed to tobacco and cigarettes smoking, alcohol consumption, and betel chewing, with a synergistic effect. In this light, the increasing awareness towards a sustainable lifestyle and a reduced use of alcohol and smoking through screening programs has produced some positive effects over time [2–5]. However, it is noteworthy that, in recent years, the diagnoses of OSCC are increasing also among people usually unexposed to these common risk factors, suggesting the implication of other factors, such as bacterial and viral infections, the diet and the genetic predisposition [6].

OSCC is usually due to the occurrence of inflammatory processes which induce alterations in cell proliferation and hence lead to chronic epithelial inflammation. Moreover, the activation of proinflammatory genes triggers the production of Reactive Oxygen Species (ROS), which contribute to alter cellular homeostasis resulting in cell damage, and promoting tumorigenesis [7]. The pro-apoptotic behavior of ROS is well known, and cells are provided with several enzymes to counteract the damages and to contrast their harmful effects. For many years, the human enzyme paraoxonase-2 (PON2), belonging to the PON family lactone hydrolyzing enzymes, attracted the attention of scientists because of its role in ROS detoxification [8–10]. The ability of PON2 enzyme to contrast ROS effects, and the enhanced efficacy of the chemotherapy treatment thanks to its knockdown has been already demonstrated in human malignant melanoma cell lines [10]. PON2 enzyme is variably expressed also in OSCC, both *in vivo* and *in vitro*, and its knockdown has been shown to significantly increase the apoptosis rate [11]. In fact, as PON2 protects healthy cells from the damage induced by free radicals, in malignant ones the effects of chemotherapy would be shielded by the action of this enzyme, defending cancer itself by the therapeutic treatment [12].

Nowadays, chemotherapy based on platinum derivatives, alone or mixed with other drugs, together with radio and immunotherapy represents one of the main treatments used for OSCC management [13,14]. Even if the choice of the treatment mostly depends on the stage of the disease, the toxicity of the drugs, and the expected outcomes, for unresectable and advanced OSCC, chemotherapy remains the golden standard, also coupled with radiotherapy in case of early stages [13]. Cisplatin (CDDP) is the best known platinum-based chemotherapy drug, with antimicrobial and antitumoral activity, used for a long time in the treatment of several types of cancer, including the OSCC [15,16]. The main CDDP mechanism of action consists of binding the N7 of purine bases leading to apoptosis through the cell cycle arrest, but, as secondary cytotoxic effects, this chemotherapy drug is also able to increase ROS production resulting in the activation of the apoptotic pathways [17].

Based on these findings, some of the Authors of this study deepened the effectiveness of CDDP in OSCC, by silencing the PON2 enzyme expression through a shRNA-mediated knockdown in HOC-621 and HSC-3 cell lines [18]. All this was made possible through a preliminary molecular investigation demonstrating firstly the high expression of the enzyme in this carcinoma, then the effective reduction of PON2, both at mRNA and at protein level (Real-time and Western blot assays) after the shRNA-mediated knockdown through the pLKO.1–647 plasmid transfection [18,19]. The success of this process was validated by the decrease in viability observed in HOC621 and HSC-3 cell lines with different time-response (respectively 48 h and 96 h). At the same time, to further enhance this promising strategy, and to ascertain the relationship between PON2 expression and CDDP resistance, chemoresistant HOC621 cell clones were generated by treating cells with increasing CDDP concentrations. In these clones, PON2 expression was demonstrated to be upregulated respect to control cells, corroborating the evidence that PON2 expression could be involved in CDDP resistance. These findings were also supported by the molecular investigation exploited by Fourier Transform InfraRed Microspectroscopy (FTIRM) which highlighted the increased oxidative damage to proteins and lipids as a result of the counteracting action of the PON2 silencing [18]. FTIRM is a high-resolution analytical technique, suitable and well-assessed in the study of cell lines, which let highlight modifications in the composition of the most relevant macromolecules (lipids, proteins, nucleic acids and carbohydrates) and detect biological spectral markers associated with specific biological mechanisms [20–22].

Based on this evidence, in the present study, FTIRM was exploited to deeply elucidate at molecular level the outcomes deriving from CDDP administration at three different time points (24, 48 and 72 h) in HOC621 and HSC-3 OSCC cell lines with PON2 silencing. IR data were analyzed by combining unsupervised multivariate and univariate statistical approaches in a full spectroscopic manner and compared with MTT results. PON2 knockdown exerted a positive effect on cisplatin efficacy in both cell lines, even if with a different response. In particular, PON2 silenced HOC 621 cells showed a less growth, respect to HSC-3 ones, at the three time points. Moreover, the statistical analysis of specific spectral markers highlighted cellular alterations mainly in nucleic acids and carbohydrates, more evident in HOC 621 ones, which therefore appeared to be more affected by chemotherapy treatment.

2. Materials and Methods

2.1. OSCC cell lines: Cultures and in-vitro treatment

The procedures involved in this work are the same as previously reported [18]. Briefly, the HOC621 and the HSC-3 human Oral Tongue Squamous Cell Carcinoma cell lines (kindly provided by Prof. Lorenzo Lo Muzio, Department of Clinical and Experimental Medicine, University of Foggia, Foggia, Italy), were transfected with pLKO.1-puro used as control and with pLKO.1–647 plasmid to perform a shRNA-mediated knockdown. The transfection process of both cell lines utilized FuGENE HD Transfection Reagent (Promega, Madison, WI, USA), according to the manufacturer's Instructions. Cells were cultured at 37 °C with 5 % CO_2 in 6-well plates ($1x10^5$ cells/well) by using a DMEM/F-12 culture medium (Dulbecco's Modified Eagle's Medium/Nutrient Ham's Mixture F-12), by the addition of 10 % FBS (Fetal Bovine Serum) and 50 μg/ml of gentamicin, up to reach enough cells to collect and to perform all experimental group in triplicate. Once the medium was replaced, HOC621 and HSC-3 cells were respectively treated with CDDP (0.25–1 μg/ml) for 24, 48, and 72 h, according to the IC_{50} values. At each time, to be harvested, cells were submitted to trypsinization and centrifuged at 500xg for 3 min at + 4°C, washed with isotonic saline solution (0.9 % NaCl), and centrifuged again. Then, cells were resuspended and fixed incubating with 500 μl of PFA (paraformaldehyde 4 %). Samples were

washed three times with 500 µl 0.9 % NaCl and resuspended in this solution (500 µl) and stored at + 4°C until FTIRM measurements. For a clear and simplified understanding, Table 1 well resumes all experimental groups investigated in this work.

2.2. MTT assay

The colorimetric assay with 3-(4,5-dimethylthiazol-2-yl)-2,5-diphenyl tetrazolium bromide (MTT) has been performed to evaluate OSCC cell viability after PON2 silencing, before and after CDDP administration [18]. To do so, cells were seeded on 96-well plates ($3x10^3$ cells/well) and then at each time point investigated, from 24 h to 72 h, 10 µl of MTT reagent (5 mg/ml in phosphate buffered saline) was dissolved in 110 µl of complete medium and added to cells (100 µl/well), incubating for 3 h at 37 °C. To lyse and to dissolve formazan crystals remained insoluble 200 µl of 2-propanol was replaced in the medium, while the amount formed during the incubation was measured in absorbance at 570 nm through an ELISA plate reader. Experiments were performed in triplicate and results of each experimental group at each time point expressed in percentage and presented as mean values ± standard deviation.

2.3. Fourier Transform InfraRed Microspectroscopy measurements

Fixed cells were washed twice with isotonic saline solution (0.9 % NaCl), resuspended in 500 µl MilliQ water and centrifuged at 800xg for 10 min each. Hence, from each sample, 15 µl of cell pellet were collected, dropped onto a CaF_2 optical window (13 mm-diameter and 1 mm-thick) and let air-dried before the acquisition in order to avoid water contributions in the IR spectra.

FTIRM analyses were performed by using a Bruker INVENIO R interferometer, coupled with a Hyperion 3000 Vis-IR microscope equipped with a HgCdTe (MCT) detector liquid nitrogen cooled (Bruker Optics, Ettlingen, Germany) with 15x objective. IR spectra were collected in transmission mode in the MIR range (4000–900 cm^{-1}) averaging 512 scans (spectral resolution 4 cm^{-1}, zero-filling factor 2, scanner velocity 40 kHz). On each sample, ~60 microareas (30 × 30 μm^2 dimension), containing groups of 3–4 densely packed cells were selected. Before each sample measurement, a clean portion of the CaF_2 window was used to acquire the background spectrum by using the same parameters.

Raw spectra collected were pre-processed through the Atmospheric Compensation and Vector-Normalization routines, respectively to remove carbon dioxide and water vapor atmospheric contribution and to normalize the full spectral range to avoid thickness variations (OPUS 7.5, Ettlingen, Germany). Pre-processed IR spectra were transformed in second derivative mode, cut in the 1310–900 cm^{-1} spectral range (representative of carbohydrates and nucleic acids) and submitted to Principal Component Analysis (PCA) (OriginPro 2023 software, OriginLab Corporation, Northampton, Massachusetts).

Finally, for each experimental group, the average absorbance spectrum, and the corresponding ± standard deviation (S.D.) spectra were calculated, for curve fitting analysis in the 1310–900 cm^{-1} spectral range. The underlying peaks were selected based on second derivative analysis and fixed before running the iterative process to obtain the best reconstructed curve (residual close to zero; bandwidth 10 to 40 cm^{-1} range) (GRAMS/AI 9.1, Galactic Industries, Inc., Salem, NH, USA). For each underlying peak, the position (in terms of wavenumbers, cm^{-1}) and the integrated area were defined, attributing the corresponding vibrational modes and biological meaning according to literature. The integrated areas of specific underlying peaks were used to calculate the following band area ratios: A_{1172}/A_{TOT} (ratio between the area of the peak at ~ 1172 cm^{-1} and the sum of the areas of all bands in the 1310–900 cm^{-1} spectral range, indicative of the presence of C-OP groups, as tumorigenic index) [23,24]; A_{1053}/A_{TOT} (ratio between the area of the peak at ~ 1053 cm^{-1} and the sum of the areas of all bands in the 1310–900 cm^{-1} spectral range; C-OH groups attributed to carbohydrates and glycosylated compounds) [21,25,26]; A_{967}/A_{1080} ratio (ratio between the areas of the peaks at ~ 967 cm^{-1} and ~ 1080 cm^{-1}; double stranded DNA backbone respect to nucleic acids phosphates) [26–28], and A_{992}/A_{TOT} (ratio between the area of the peak at ~ 992 cm^{-1} and the sum of the areas of all bands in the 1310–900 cm^{-1} spectral range; C-O ribose moieties attributable to RNA) [20,26,27].

2.4. Statistical analysis

Data are reported as mean ± S.D (Standard Deviation). The statistical analysis was performed by using GraphPad Prism software version 8.00 for Windows (GraphPad Software, San Diego, CA, USA). One-way analysis of variance (ANOVA) and *Student t-test* were adopted respectively to evaluate statistically significant differences for both cell lines between (i) cells transfected with the *p. puro* and *p. 647* plasmids among all time points considered (at 24, 48, and 72 h), and (ii) for the comparison between *p. puro* an *p. 647* transfected cell lines, at each time point recorded. Statistical significance was set at $p < 0.05$. Different letters over the histograms mean statistically significant differences of One-way ANOVA submitted groups, while asterisks over there reported the statistical significance among groups submitted to Student's *t-test*.

3. Results

3.1. Cell viability assay

Previous Real-time PCR analyses demonstrated a significant decrease of PON2 mRNA levels in HSC-3 cells transfected with pLKO.1–647 (0.3435 ± 0.0013; p = 0.0010) compared with pLKO.1-puro (1.0000 ±

Table 1
Experimental groups. The CDDP doses administered to HOC621 and HSC-3 cell lines were respectively 1 µg/ml and 0.25 µg/ml.

Cell line	Time points (hours)	pLKO.1-puro		Relative PON2 mRNA expression	pLKO.1–647		Relative PON2 mRNA expression
		No CDDP	CDDP		No CDDP	CDDP	
HOC621	**24**	HOC p. puro 24 h	HOC p. puro CDDP 24 h		HOC p. 647 24 h	HOC p. 647 CDDP 24 h	
	48	HOC p. puro 48 h	HOC p. puro CDDP 48 h	1.0000 ± 0.1631	HOC p. 647 48 h	HOC p. 647 CDDP 48 h	0.5864 ± 0.0660
	72	HOC p. puro 72 h	HOC p. puro CDDP 724 h		HOC p. 647 72 h	HOC p. 647 CDDP 72 h	
HSC-3	**24**	HSC3 p. puro 24 h	HSC3 p. puro CDDP 24 h		HSC3 p. 647 24 h	HSC3 p. 647 CDDP 24 h	
	48	HSC3 p. puro 48 h	HSC3 p. puro CDDP 48 h	1.0000 ± 0.1220	HSC3 p. 647 48 h	HSC3 p. 647 CDDP 48 h	0.3435 ± 0.0013
	72	HSC3 p. puro 72 h	HSC3 p. puro CDDP 72 h		HSC3 p. 647 72 h	HSC3 p. 647 CDDP 72 h	

0.1220); analogously, in HOC621 cell line, treatment with pLKO.1–647 (0.5864 ± 0.0660; p = 0.0352) led to a significant reduction of enzyme expression compared with pLKO.1-puro (1.0000 ± 0.1631) [18].

The MTT assay was performed to evaluate cell viability, after the following treatments: transfection with the p. puro and p. 647 plasmids (HOC621, Fig. 1A; HSC-3, Fig. 1D); transfection with the p. puro plasmid and before and after the CDDP administration (HOC621, Fig. 1B; HSC-3, Fig. 1E); transfection with the p.647 plasmid and before and after the CDDP administration (HOC621, Fig. 1C; HSC-3, Fig. 1F). In general, a different response, both in terms of percentage of viable cells and timing was observed: in fact, HSC-3 cells seem to be less affected by CDDP treatment than HOC621 ones, showing a slower growth. What emerged highlights a more rapid increase in p. puro HOC compared to p. puro HSC-3, which resulted in both cases reduced by the transfection with p.647: this was more evident and in a more timely fashion in HOC621 than in HSC-3 (Fig. 1A,D). The efficacy of Cisplatin is demonstrated by the decreasing in cell viability, more evident in both p.647 cell lines (Fig. 1C,F) than in p. puro ones (Fig. 1B,E), where more marked results were showed only after 72 h especially in HOC621 cells. This time-response was reduced in p.647, as a consequence of the PON2 silencing, and the effects exerted by the drug were evidenced earlier (Fig. 1C,F).

3.2. FTIRM analyses

A representative absorbance spectrum of a cellular sample is reported in Fig. 2 both in absorbance and second derivative mode. The investigated spectral range is 1310–900 cm^{-1}, meaningful for nucleic acids and carbohydrates. The most significant peaks are listed in Table 2, together with the associated vibrational modes and the biological meaning.

The spectra of HOC621 and HSC-3 cell lines were first submitted to the unsupervised Principal Component Analysis (PCA), to first highlight the effects due to both the transfection processes and the CDDP treatment.

The PCA scores plots of HOC621 cell populations transfected with the two plasmids (p. puro, Fig. 3A–G; p. 647, Fig. 3H–N) before and after CDDP treatment are analyzed below.

As regard not silenced HOC621cells (HOC p. puro), the PCA scores plot calculated on all the spectral populations (Fig. 3A) evidenced a separation between CDDP treated and not treated cells at all time points along PC2 axis (explained variance 25.4 %); moreover, an almost complete superimposition was found in not treated cells at all time points (HOC p. puro 24 h; HOC p. puro 48 h, and HOC p. puro 72 h), while as regards CDDP treated ones, a superimposition was found only at 24 h and 48 h of treatment (HOC p. puro CDDP 24 h, and HOC p. puro CDDP 48 h), respect to 72 h (HOC p. puro CDDP 72 h), which resulted slightly separated along PC1 axis (explained variance 33.1 %). The pairwise comparisons between CDDP treated and not treated cells evidenced a complete segregation along PC1 axis at each time point (HOC p. puro 24 h *vs* HOC p. puro CDDP 24 h, Fig. 3B; HOC p. puro 48 h *vs* HOC p. puro CDDP 48 h, Fig. 3C, and HOC p. puro 72 h *vs* HOC p. puro CDDP 72 h, Fig. 3D), with explained variances higher than 40 %. The analysis of the relative loadings let identify the main spectral differences explaining the segregation (Fig. 3E–G).

A similar trend was shown by PON2 silenced HOC621 cells (HOC p. 647); some overlapping was found at all time points within not treated cells (HOC p. 647 24 h; HOC p. 647 48 h, and HOC p. 647 72 h) and within CDDP treated ones (HOC p. 647 CDDP 24 h; HOC p. 647 CDDP 48 h, and HOC p. 647 CDDP 72 h); the two groups are however separated one from the other along PC2 axis (explained variance 29.6 %) (Fig. 3H). Also in this case, a well evident segregation between CDDP treated and not treated silenced cells was highlighted at each time point by the pairwise comparisons (HOC p. 647 24 h *vs* HOC p. 647 CDDP 24 h, Fig. 3I; HOC p. 647 48 h *vs* HOC p. 647 CDDP 48 h, Fig. 3J, and HOC p. 647 72 h *vs* HOC p. 647 CDDP 72 h, Fig. 3K), with explained variances higher than 44 %. The analysis of the relative loadings let identify the main spectral differences explaining the segregation (Fig. 3L-N).

As for the HOC621 cell line, the same multivariate approach was exploited for HSC-3 one (p. puro, Fig. 4A–G; p. 647, Fig. 4H–N). Here, the situation is quite different respect to the one observed in HOC621 cells: in fact, HSC-3 cells, due to their different behavior already shown by the vitality test, seem to show the consequences induced by CDDP later on, demonstrating to be more resistant respect to the HOC621 line.

As reported in Fig. 4A, not silenced HSC-3 cells are quite well divided along PC1 axis between not treated and CDDP treated ones (explained variance 28.3 %), and along the PC2 axis (explained variance 10.5 %) between the first time point (HSC-3p. puro 24 h and HSC-3p. puro CDDP 24 h) and the other two (HSC-3p. puro 48 h, HSC-3p. puro 72, HSC-3p. puro CDDP 48 h, and HSC-3p. puro CDDP 72). A complete superimposition between 48 h and 72 h CDDP treated cells (HSC-3p. puro CDDP 48 h and HSC-3p. puro CDDP 72 h) and 48 h e 72 h not treated ones (HSC-3p. puro 48 h and HSC-3p. puro 72 h) was observed. After the PON2 silencing, the segregation along the PC1 axis (explained variance 36.6 %) is more noticeable between CDDP-treated (HSC-3p. 647 CDDP 24 h, HSC-3p. 647 CDDP 48 h, and HSC-3p. 647 CDDP 48 h) and not treated

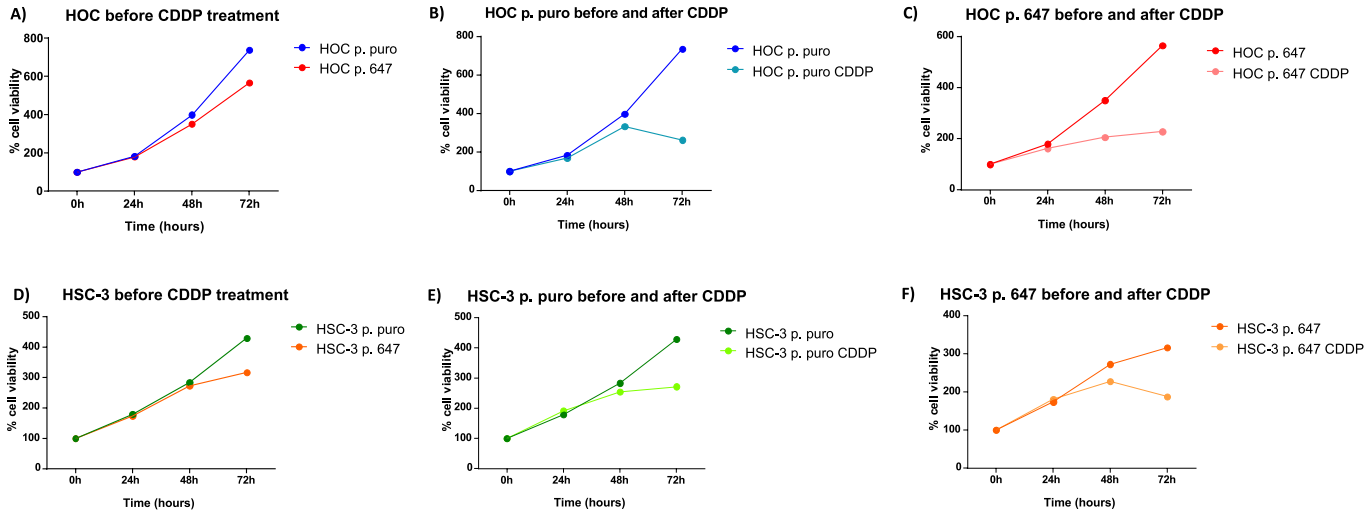

Fig. 1. MTT assays performed on HOC621 cell line (**A,B,C**) and HSC-3 (**D,E,F**); comparison between % of cell viability between: **A,D**) p. puro and p. 647 transfected cells; **B,E**) p. puro and p. puro – CDDP; and **C,F**) p. 647 and p. 647 – CDDP.

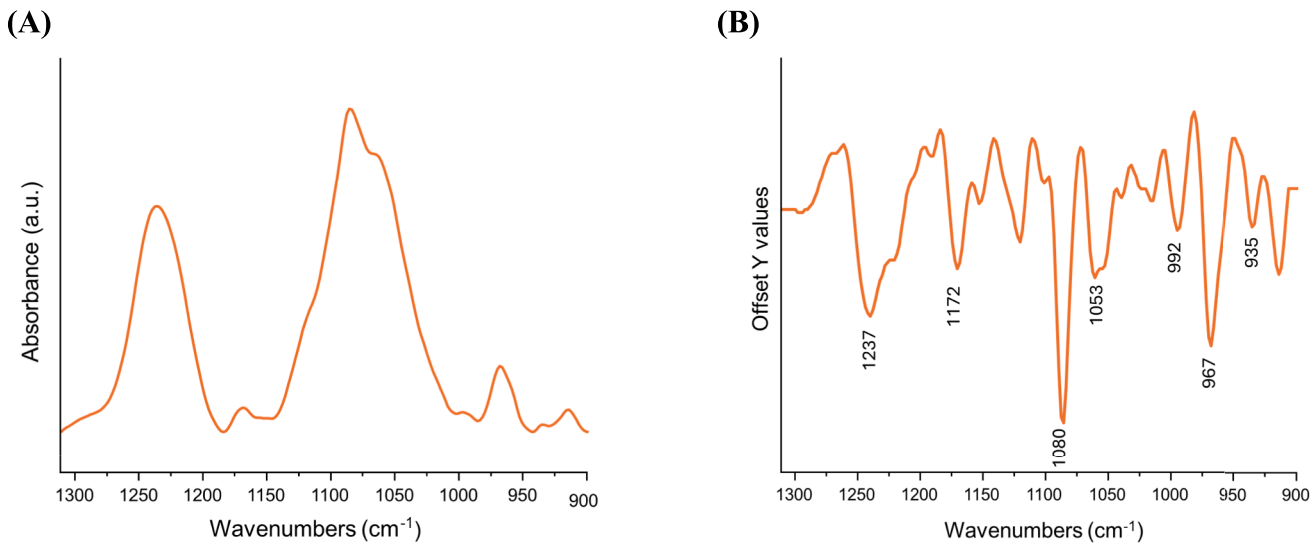

Fig. 2. A representative IR spectrum of a cellular sample showed in the 1310–900 cm^{-1} spectral range both in absorbance (A) and second derivative (B) modes.

Table 2
Meaningful IR absorptions of a cellular sample: position (wavenumbers), associated vibrational mode and cellular component.

Position (wavenumbers, cm^{-1})	Vibrational modes and cellular components
~1237, and ~ 1080	Asymmetric and symmetric stretching vibration of PO_2^- groups (ν_{asym} PO_2^- and ν_{sym} PO_2^-) in nucleic acids
~1172	Tumorigenic index
~1053	Stretching of C-O-C and C-OH moieties in carbohydrates
~992	Stretching of C–C and C-O in RNA ribose ring breathing
~967	Backbone vibration of nucleic acids in double strand DNA
~935	Vibration in Z DNA

cells (HSC-3p. 647 24 h, HSC-3p. 647 48 h, and HSC-3p. 647 48 h) (Fig. 4H). The pairwise PCA comparisons highlighted a defined segregation at each time point, between CDDP treated and not treated cells both in HSC-3p. puro (explained variance higher than 26 %; Fig. 4B–D) and p.647 (explained variance higher than 36 %; Fig. 4I–K) cells, with loadings explaining the main spectral differences responsible of these separations (p. puro, Fig. 4E–G, and p.647, Fig. 4L–N).

MTT analysis clearly demonstrated that cells transfected with p.647 plasmid, and hence PON2 silenced, better respond to CDDP treatment respect to not silenced ones, and that, in most cases, not CDDP treated cells did not show significant results, especially in HOC621 cell line. In this light, the univariate analysis described below only was performed only on cells after CDDP administration, in order to focus the attention on the variability expressed by both cell lines in relation with the chemotherapy treatment. In this light, to better highlight the biological modifications induced by the transfection as well as by the CDDP treatment, specific band area ratios were investigated. In Fig. 5, the statistical analysis of these spectral parameters calculated on both HOC621 and HSC-3 cell lines is reported. The A_{1172}/A_{TOT} represents a tumorigenic index and is a malignant spectral marker related to phosphorylated C-O groups [29]; the values of this marker were higher in HSC-3 cells than HOC621ones. In HOC621 cells, a time related decreasing trend was observed, with lower levels in PON2 silenced cells than in not silenced ones; in HSC-3, the decrease was only observed in p.647 cells over time with statistically significant values, while in p. puro levels are not significantly unchanged. This slowdown evidenced once again the more aggressive behavior of HSC-3 and the faster response of HOC621 cells. The metabolic pattern was evaluated through the investigation of the A_{1053}/A_{TOT} ratio, representative of performance exerted by carbohydrates. The efficacy of CDDP and the slowdown due to the cell cycle arrest was more evident by the decrease occurred in p.647 respect to p. puro in HOC621 cells, while in HSC-3 especially after 72 h, even with no statistically significant differences at each time point analyzed between not PON2 silenced and silenced cells. Moving to ratios representative of nucleic acids, the A_{967}/A_{1080} ratio, explaining the total amount of DNA, evidenced that HOC621 p. puro cells seem to have a significant increase over time differently from p. 647 cells which showed a decreasing trend after 48 and 72 h, contraposing to the increasing one observed in p. puro, suggesting different effects induced by the chemotherapy administration. Conversely, in HSC-3 the decrease progresses as slowly with no statistical significance, both in p. puro and in p.647. Finally, and according to the just mentioned DNA, the RNA level measured with the A_{992}/A_{TOT} ratio, confirmed the trend of a more evident transcription arrest in PON2 silenced cells especially after 48 h in HOC621 and to a greater extent in HSC-3.

4. Discussion

Cancer continues to be among the most frequent cause of death worldwide, and the OSCC is one of the most recurrent and invasive cancers involving the head and neck district. Despite all the innovative therapies alongside the traditional cures, such as the chemotherapy, drug-resistance mechanisms contribute to treatment failure and then to worse prognosis [30]. This drawback could be ascribed to several factors, from the unsuccessful entry of the drug inside the cell or its inactivation, to the role exerted by the Tumor Microenvironment and by the Epithelial Mesenchymal Transition, including the DNA Damage Response (DDR) just to name a few [31]. It has been demonstrated that the processes involved in the redox homeostasis could be altered in cancer cells, and the redox-mediated mechanisms of chemoresistance can lead to improving cancer fitness through the progression of cell-cycle and the enhancement of metastatic behavior [32]. In this light, the Paraoxonase-2 (PON2) enzyme takes on a role in defending cells by the actions of Reactive Oxygen Species (ROS). This intracellular enzyme, belonging to the PON enzyme family is localized on several intracellular membranes, is highly expressed in various human tissues, and is involved in some neoplasms, ensuring the correct function of the electron transport chain, reducing oxygen species, and maintaining cellular homeostasis [8]. The ability of this enzyme to act against ROS faces off with the CDDP mechanism of action. In fact, despite the first step of the drug in binding the purine bases N7 once internalized in cells, the increased oxidative damage provoked by the activation of the resulting apoptotic pathways met the role of those enzymes involved in reducing

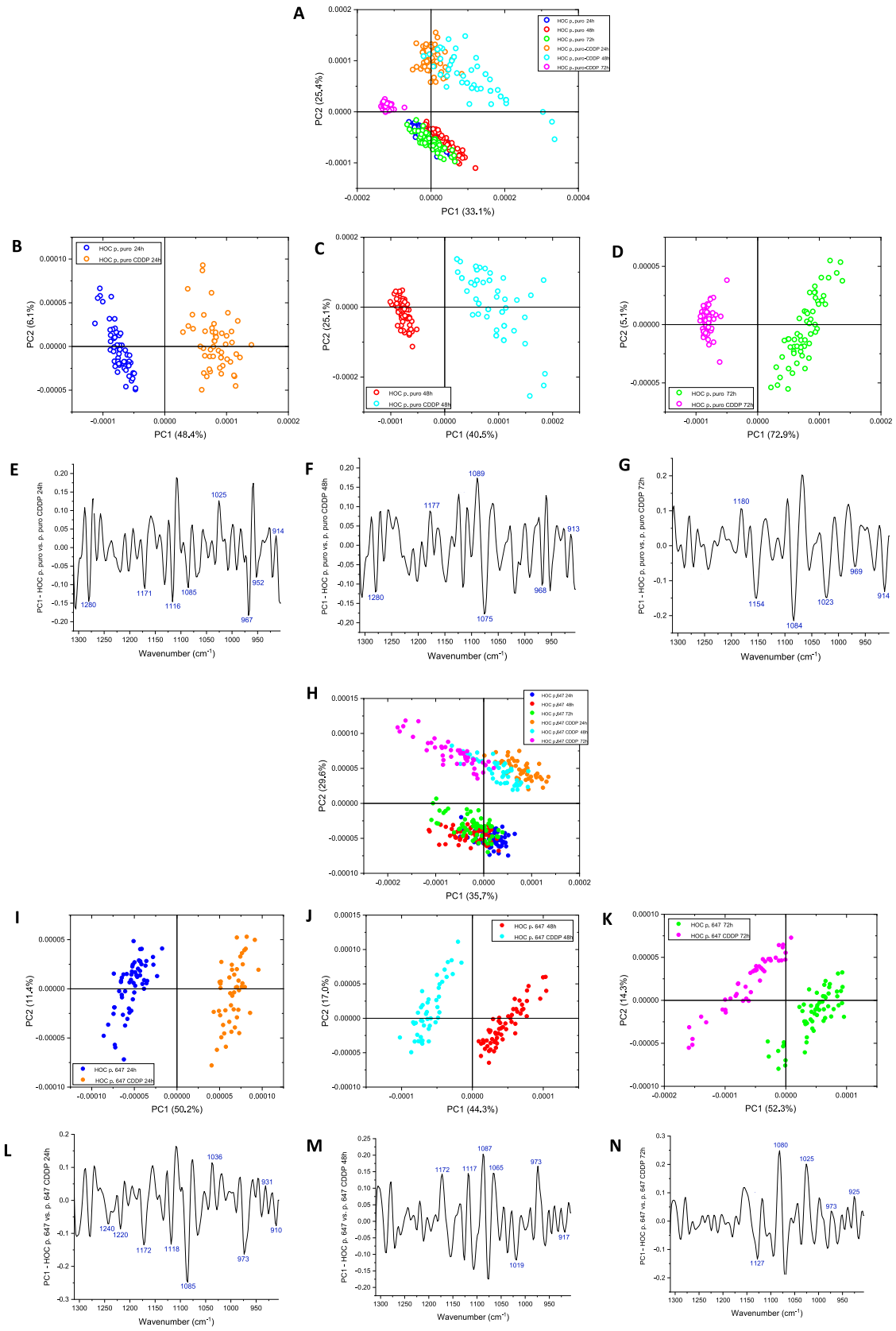

Fig. 3. PCA analysis performed in the 1310–900 cm^{-1} spectral range on HOC621 cells transfected with p. puro (A-G) and p. 647 (H-N), with and without CDDP treatment.

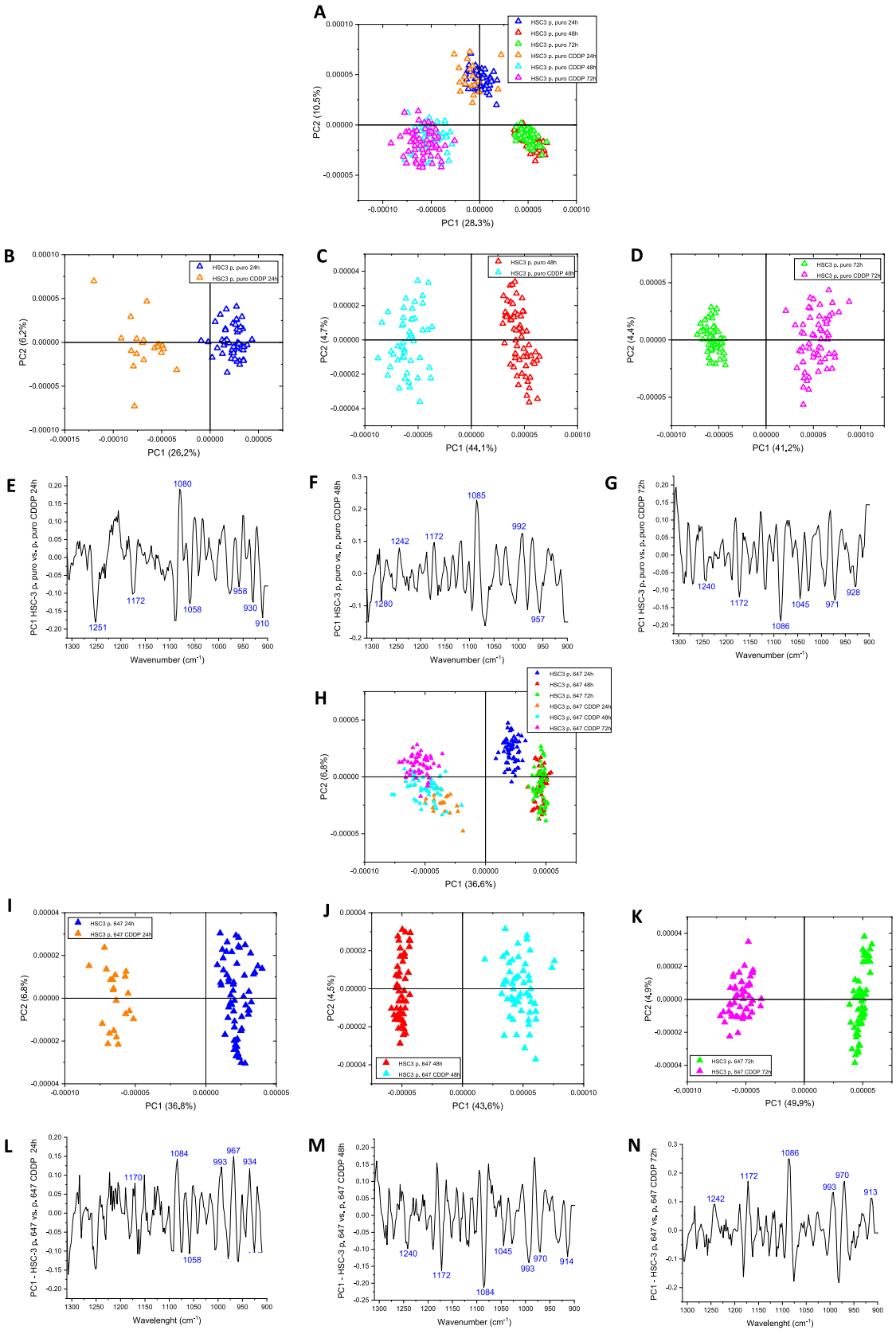

Fig. 4. PCA analysis performed in the 1310–900 cm^{-1} spectral range on HSC-3 cells transfected with p. puro (A-G) and p. 647 (H-N) with and without CDDP treatment.

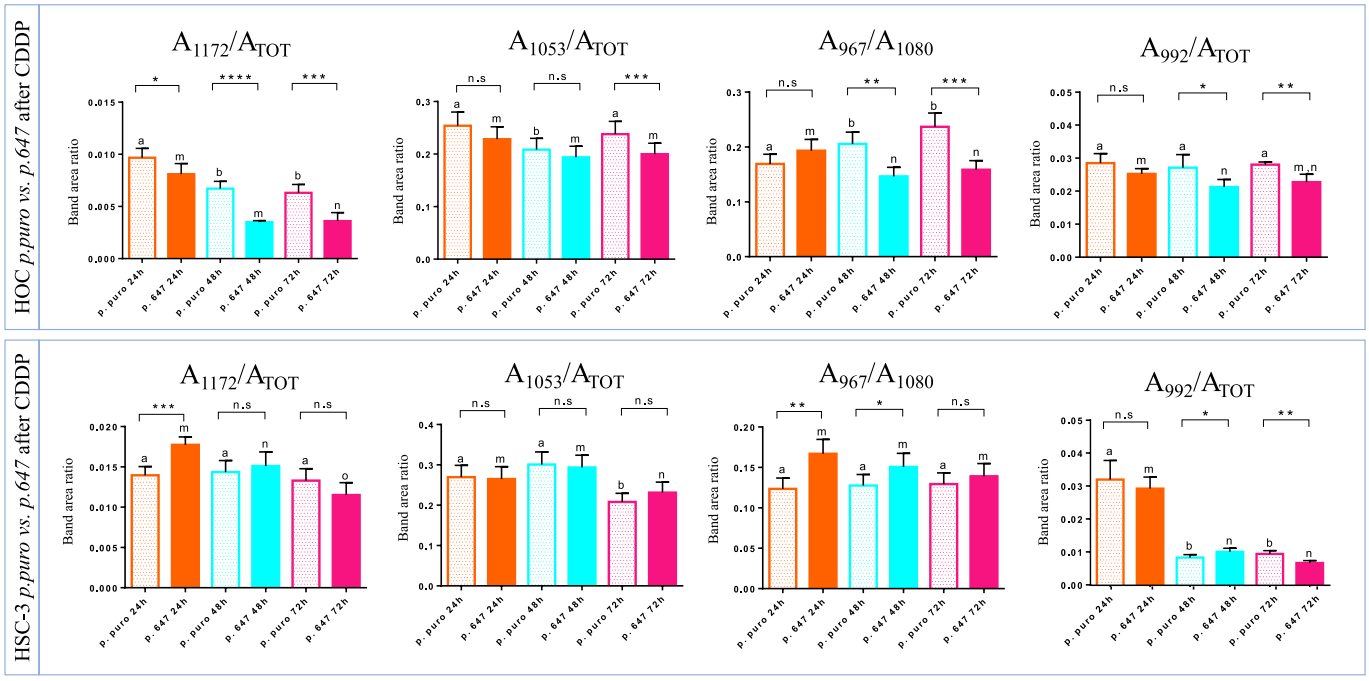

Fig. 5. Band/area ratios calculated for HOC621 and HSC-3 cell lines comparing p. puro and p.647 transfected cells after CDDP treatment. Statistical significance was set at $p < 0.05$. Different letters over the histograms mean statistically significant differences of one-way ANOVA submitted groups, while asterisks over there reported the statistical significance among groups submitted to *t*-test ($p > 0.05$n.s; $p < 0.05$ *; $p < 0.01$ **; $p < 0.001$ ***; $p < 0.0001$ ****).

the oxidative stress and was responsible of cellular homeostasis, like the PON2. In this way, the natural role of PON2 affects the efficacy of the chemotherapy, making cells resistant.

The chemoresistance promoted by the presence of the PON2 constitutes the pillar around which revolves the purpose of this work. As previously reported by the same authors [18] the efficacy of CDDP treatment has been improved by the silencing of PON2 expression through the transfection of HOC621 and HSC-3 cell lines with pLKO.1–647 plasmid containing the shRNA able to knockdown the enzyme expression. In this way, avoiding its expression and hence its functionality, the damage resulting from CDDP treatment has not been shielded by its action. Upon entering the cell, a hydrolytic displacement of chloride atoms in CDDP molecule occurs, generating a strong electrophilic species which promptly reacts with nitrogen atoms and protein sulfhydryl groups of nucleic acid bases. In detail, CDDP can bind the N7 of purine bases resulting in DNA structural damage, which triggers cell cycle arrest and further apoptotic pathway initiation. However, CDDP can exert its cytotoxic activity also boosting ROS release. Indeed, upon entering cancer cell, CDDP is responsible for a massive ROS production which contributes damaging DNA resulting in the apoptotic pathway activation [17].

In this first work, the Fourier Transform InfraRed Microspectroscopy (FTIRM) assumed a secondary role affirming the success of CDDP treatment after the PON2 silencing in HOC621 and HSC-3 cells. The comparison between CDDP-treated PON2 silenced cells (transfected with pLKO.1–647 plasmid) and not silenced cells (transfected with pLKO.1 puro plasmid) suggested an increased level of spectral biomarkers related to the oxidative stress damage exerted on lipids and proteins, in both cell lines, with marked evidence in down-regulated PON2 cells (pLKO.1 647) respect to the not silenced controls (pLKO.1 puro) [18].

Starting from these findings the aim of the current study was to further investigate the role exerted by CDDP after the PON2 knockdown by using exclusively a FTIRM approach. In this case, in fact, HOC621 and HSC-3 cells were further investigated individually, at three distinct time points (24, 48, 72 h after CDDP treatment) by employing the unsupervised Principal Component Analysis (PCA) to first detect differences occurring after the transfection with both plasmids, and hence after CDDP administration maintaining the same doses respectively used in the previous work. What emerges evidenced a different response between HOC621 and HSC-3, as initially reported by the MTT assay. In fact, HOC621 cell line showed the highest percentage of cell viability respect to HSC-3 ones; therefore, especially in HOC cell line, cells transfected with p. 647 demonstrated to grow less respect to those not PON2 silenced (pLKO.1 puro) in both cell lines, suggesting a first weakening action. The effects exerted by the CDDP administration affected more HOC621 than HSC-3 since the earlier time points, implying an increased sensitivity to chemotherapy drugs. The divergence arising between HOC621 and HSC-3 consisted also in the different time-response. While HOC621 cell line showed the effects after the first time point considered (after 24 h), HSC-3 resulted in a slower efficacy (after 48 h) as well evidenced by MTT assays and then by PCA. These outcomes explained the variability played by these oral squamous cell carcinoma cells to act otherwise as a consequence of the same stimulus.

Thus, based on these results, the band area ratios were analyzed mainly considering representative carbohydrates, DNA and RNA ratio, including the tumorigenic index one. The results of this semi-quantitative evaluation were consistent with the previously observed ones highlighting both the stronger efficacy of CDDP in p.647 transfected cells, and hence PON2 silenced, respect to those transfected with the empty plasmid p. puro, and, in addition, the highest sensibility expressed by the HOC621 cell line than that showed by the HSC-3.

At this point, the investigative approach used in this work, as in the previous one, contributed to shedding new light on the chemoresistance mechanism in which PON2 enzyme expression seems to be involved, also showing different time responses and variability displayed by two different cell lines descending from Oral Tongue Squamous Cell Carcinoma.

5. Conclusion

The in *vitro* knockdown of PON2 expression mediated by the shRNA in OTSCC cell lines showed to be an excellent strategy to repress the CDDP chemoresistance. Despite the previous results obtained, the

improved efficacy of the chemotherapy after the PON2 silencing has been demonstrated again through a full FTIRM vibrational spectroscopic approach, which, coupling the multivariate and the univariate statistical tools, lead to meaningful responses from two different cell lines investigated. The different results obtained by both cells evidenced the possible variability existing in this oral carcinoma, suggesting potential implications occurring even in an enhanced chemotherapy strategy.

CRediT authorship contribution statement

Alessia Belloni: Formal analysis, Investigation, Methodology, Software, Visualization, Writing – original draft. **Roberto Campagna:** Formal analysis, Investigation, Methodology, Visualization, Writing – original draft. **Valentina Notarstefano:** Formal analysis, Investigation, Methodology, Software, Visualization, Writing – original draft. **Valentina Pozzi:** Investigation, Validation, Visualization. **Giulia Orilisi:** Visualization, Writing – original draft. **Veronica Pompei:** Writing – review & editing. **Lucrezia Togni:** Writing – original draft. **Marco Mascitti:** Conceptualization. **Davide Sartini:** Conceptualization, Methodology, Project administration, Supervision, Validation, Writing – review & editing. **Elisabetta Giorgini:** Conceptualization, Methodology, Project administration, Supervision, Validation, Writing – review & editing. **Andrea Santarelli:** Conceptualization, Supervision, Writing – review & editing. **Monica Emanuelli:** Conceptualization, Project administration, Supervision, Validation, Writing – review & editing.

Funding

This research did not receive any specific grant from funding agencies in the public, commercial, or not-for-profit sectors.

Declaration of competing interest

The authors declare that they have no known competing financial interests or personal relationships that could have appeared to influence the work reported in this paper.

Data availability

Data will be made available on request.

References

[1] H. Sung, J. Ferlay, R.L. Siegel, M. Laversanne, I. Soerjomataram, A. Jemal, F. Bray, Global Cancer Statistics, GLOBOCAN Estimates of Incidence and Mortality Worldwide for 36 Cancers in 185 Countries, CA A Cancer J Clinicians 71 (2021) (2020) 209–249, https://doi.org/10.3322/caac.21660.

[2] M. Ansarin, R. De Berardinis, F. Corso, G. Giugliano, R. Bruschini, L. De Benedetto, S. Zorzi, F. Maffini, F. Sovardi, C. Pigni, D. Scaglione, D. Alterio, M. Cossu Rocca, S. Chiocca, S. Gandini, M. Tagliabue, Survival Outcomes in Oral Tongue Cancer: A Mono-Institutional Experience Focusing on Age, Front. Oncol. 11 (2021) 616653, https://doi.org/10.3389/fonc.2021.616653.

[3] C. Hung, C. Chien, P. Chu, Y. Wu, C. Lin, C. Huang, L. Chan, Y. Wang, S.F. Yuan, T. Hour, J.Y. Chen, Differential resistance to platinum-based drugs and 5-fluorouracil in p22phox-overexpressing oral squamous cell carcinoma: Implications of alternative treatment strategies, Head Neck 39 (2017) 1621–1630, https://doi.org/10.1002/hed.24803.

[4] D.R. Farquhar, A.M. Tanner, M.M. Masood, S.R. Patel, T.G. Hackman, A.F. Olshan, A.L. Mazul, J.P. Zevallos, Oral tongue carcinoma among young patients: An analysis of risk factors and survival, Oral Oncol. 84 (2018) 7–11, https://doi.org/10.1016/j.oraloncology.2018.06.014.

[5] J.-P. Foy, C. Bertolus, D. Boutolleau, H. Agut, A. Gessain, Z. Herceg, P. Saintigny, Arguments to Support a Viral Origin of Oral Squamous Cell Carcinoma in Non-Smoker and Non-Drinker Patients, Front. Oncol. 10 (2020) 822, https://doi.org/10.3389/fonc.2020.00822.

[6] S. Irani, New Insights into Oral Cancer—Risk Factors and Prevention: A Review of Literature, Int. J. Prev. Med. 11 (2020) 202, https://doi.org/10.4103/ijpvm.IJPVM.

[7] F. Pezzuto, L. Buonaguro, F. Caponigro, F. Ionna, N. Starita, C. Annunziata, F. M. Buonaguro, M.L. Tornesello, Update on head and neck cancer: Current knowledge on epidemiology, risk factors, molecular features and novel therapies, Oncology (switzerland) 89 (2015) 125–136, https://doi.org/10.1159/000381717.

[8] T. Bacchetti, G. Ferretti, A. Sahebkar, The role of paraoxonase in cancer, Semin. Cancer Biol. 56 (2019) 72–86, https://doi.org/10.1016/j.semcancer.2017.11.013.

[9] G. Manco, E. Porzio, T.M. Carusone, Human paraoxonase-2 (Pon2): Protein functions and modulation, Antioxidants 10 (2021) 1–28, https://doi.org/10.3390/antiox10020256.

[10] R. Campagna, T. Bacchetti, E. Salvolini, V. Pozzi, E. Molinelli, V. Brisigotti, D. Sartini, A. Campanati, G. Ferretti, A. Offidani, M. Emanuelli, Paraoxonase-2 silencing enhances sensitivity of a375 melanoma cells to treatment with cisplatin, Antioxidants 9 (2020) 1–13, https://doi.org/10.3390/antiox9121238.

[11] M. Krüger, J. Amort, P. Wilgenbus, J.P. Helmstädter, I. Grechowa, J. Ebert, S. Tenzer, M. Moergel, I. Witte, S. Horke, The anti-apoptotic PON2 protein is Wnt / β-catenin-regulated and correlates with radiotherapy resistance in OSCC patients, Oncotarget 7 (2016).

[12] S.M.R.T. Sepideh Mirzaei, K. Hushmandi, A. Zabolian, S.O.S. Hossein Saleki, A. Ranjbar, A.Z. SeyedHesam SeyedSaleh, K.A. Haroon Khan, Milad Ashrafizadeh, Elucidating Role of Reactive Oxygen Species (ROS) in Cisplatin Chemotherapy : A Focus on Molecular Pathways and Possible, Molecules MDPI 26 (2021) 2382, https://doi.org/10.3390/molecules26082382.

[13] J. Noguti, C.F.G. De Moura, G.P.P. De Jesus, V.H.P. Da Silva, T.A. Hossaka, C.T. F. Oshima, D.A. Ribeiro, Metastasis from oral cancer: An overview, Cancer Genomics Proteomics 9 (2012) 329–336.

[14] S. Schmitz, K.K. Ang, J. Vermorken, R. Haddad, C. Suarez, G.T. Wolf, M. Hamoir, J. P. Machiels, Targeted therapies for squamous cell carcinoma of the head and neck: Current knowledge and future directions, Cancer Treat. Rev. 40 (2014) 390–404, https://doi.org/10.1016/j.ctrv.2013.09.007.

[15] A. Eastman, The Mechanism of Action of Cisplatin: From Adducts to Apoptosis, in: B. Lippert (Ed.), Cisplatin, 1st ed.,, Wiley, 1999, pp. 111–134, https://doi.org/10.1002/9783906390420.ch4.

[16] K. Joyce, S. Saxena, A. Williams, C. Damurjian, N. Auricchio, S. Aluotto, H. Tynan, A.L. Demain, Antimicrobial spectrum of the antitumor agent, cisplatin, J Antibiot 63 (2010) 530–532, https://doi.org/10.1038/ja.2010.64.

[17] S. Dasari, P. Bernard Tchounwou, Cisplatin in cancer therapy: Molecular mechanisms of action, European Journal of Pharmacology 740 (2014) 364–378, https://doi.org/10.1016/j.ejphar.2014.07.025.

[18] R. Campagna, A. Belloni, V. Pozzi, A. Salvucci, V. Notarstefano, L. Togni, M. Mascitti, D. Sartini, E. Giorgini, E. Salvolini, A. Santarelli, L. Lo Muzio, M. Emanuelli, Role Played by Paraoxonase-2 Enzyme in Cell Viability , Proliferation and Sensitivity to Chemotherapy of Oral Squamous Cell Carcinoma Cell Lines, International Journal of Molecular Sciences - MDPI 24 (2023) 338, https://doi.org/10.3390/ijms24010338.

[19] R. Campagna, V. Pozzi, A. Salvucci, L. Togni, M. Mascitti, D. Sartini, E. Salvolini, A. Santarelli, L. Lo Muzio, M. Emanuelli, Paraoxonase-2 expression in oral squamous cell carcinoma, Hum. Cell 36 (2023) 1211–1213, https://doi.org/10.1007/s13577-023-00875-w.

[20] E. Giorgini, S. Sabbatini, R. Rocchetti, V. Notarstefano, C. Rubini, C. Conti, G. Orilisi, E. Mitri, D.E. Bedolla, L. Vaccari, In vitro FTIR microspectroscopy analysis of primary oral squamous carcinoma cells treated with cisplatin and 5-fluorouracil: A new spectroscopic approach for studying the drug-cell interaction, Analyst 143 (2018) 3317–3326, https://doi.org/10.1039/c8an00602d.

[21] V. Notarstefano, S. Sabbatini, C. Pro, A. Belloni, L.V. Giulia Orilisi, C. Rubini, H. J. Byrne, E.G. And, Exploiting fourier transform infrared and Raman microspectroscopies on cancer stem cells from oral squamous cells carcinoma : new evidence of acquired cisplatin chemoresistance, Analyst 145 (2020) 8038–8049, https://doi.org/10.1039/d0an01623c.

[22] V. Notarstefano, A. Belloni, S. Sabbatini, C. Pro, G. Orilisi, R. Monterubbianesi, V. Tosco, H.J. Byrne, L. Vaccari, E. Giorgini, Cytotoxic Effects of 5-Azacytidine on Primary Tumour Cells and Cancer Stem Cells from Oral Squamous Cell Carcinoma : An In Vitro FTIRM Analysis, Cells (2021), https://doi.org/10.3390/cells10082127.

[23] B. Vileno, S. Jeney, A. Sienkiewicz, P.R. Marcoux, L.M. Miller, L. Forró, Evidence of lipid peroxidation and protein phosphorylation in cells upon oxidative stress photo-generated by fullerols, Biophys. Chem. 152 (2010) 164–169, https://doi.org/10.1016/j.bpc.2010.09.004.

[24] P.K. Davis, G.V. Johnson, Energy metabolism and protein phosphorylation during apoptosis: a phosphorylation study of tau and high-molecular-weight tau in differentiated PC12 cells, Biochem. J. 340 (1999) 51–58.

[25] V. Notarstefano, G. Gioacchini, E. Giorgini, N. Montik, A. Ciavattini, A.R. Polidori, F.A. Candela, L. Vaccari, M. Cignitti, O. Carnevali, The Impact of Controlled Ovarian Stimulation Hormones on the Metabolic State and Endocannabinoid System of Human Cumulus Cells, Int. J. Mol. Sci. 21 (2020) 7124, https://doi.org/10.3390/ijms21197124.

[26] A.C.S. Talari, M.A.G. Martinez, Z. Movasaghi, S. Rehman, I.U. Rehman, Advances in Fourier transform infrared (FTIR) spectroscopy of biological tissues, Appl. Spectrosc. Rev. 52 (2017) 456–506, https://doi.org/10.1080/05704928.2016.1230863.

[27] P. Zucchiatti, E. Mitri, S. Kenig, F. Bille, G. Kourousias, D.E. Bedolla, L. Vaccari, Contribution of Ribonucleic Acid (RNA) to the fourier transform infrared (FTIR) Spectrum of eukaryotic cells, Anal. Chem. 88 (2016) 12090–12098, https://doi.org/10.1021/acs.analchem.6b02744.

[28] G. Gioacchini, V. Notarstefano, E. Sereni, C. Zacà, G. Coticchio, E. Giorgini, L. Vaccari, O. Carnevali, A. Borini, Does the molecular and metabolic profile of human granulosa cells correlate with oocyte fate? New Insights by Fourier Transform Infrared Microspectroscopy Analysis, MHR: Basic Science of Reproductive Medicine 24 (2018) 521–532, https://doi.org/10.1093/molehr/gay035.

[29] M. Banyay, M. Sarkar, A. Gräslund, A library of IR bands of nucleic acids in solution, Biophys. Chem. 104 (2003) 477–488, https://doi.org/10.1016/S0301-4622(03)00035-8.
[30] Y. Kanno, C.-Y. Chen, H.-L. Lee, J.-F. Chiou, Y.-J. Chen, Molecular Mechanisms of Chemotherapy Resistance in Head and Neck Cancers, Front. Oncol. 11 (2021), https://doi.org/10.3389/fonc.2021.640392.
[31] A. Ramos, S. Sadeghi, H. Tabatabaeian, Battling chemoresistance in cancer: Root causes and strategies to uproot them, Int. J. Mol. Sci. 22 (2021) 1–22, https://doi.org/10.3390/ijms22179451.
[32] E.K. Kim, M. Jang, M.J. Song, D. Kim, Y. Kim, H.H. Jang, Redox-mediated mechanism of chemoresistance in cancer cells, Antioxidants 8 (2019), https://doi.org/10.3390/antiox8100471.